Electrochemical investigations of a substituted oxidation stable polypyrrole

W. A. Goedel*, G. Hölz and G. Wegner
Max-Planck-Institut für Polymerforschung, Ackermannweg 10, 6500 Mainz, Germany

and J. Rosenmund
Institut für Physikalische Chemie, Universität Kiel, 2300 Kiel, Germany

and G. Zotti
Consiglio Nazionale delle Ricerche, Istituto di Polarografia ed Elettrochimica Preparativa, Corso Stati Uniti 4, 35020 Padua, Italy
(Received 18 January 1993)

The polar substituted polypyrrole, poly(5-acetamido-4,5,6,7-tetrahydro-2*H*-benzo[c]pyrrole), can be oxidized up to a degree of oxidation of 0.8 charges per pyrrole ring without substantial degradation. Its cyclic voltammogram (CV) shows two redox peaks. Variation of the sweep rate of the CVs and *in situ* gravimetric experiments show that the second anodic peak is associated with a swelling of the polymer. *In situ* u.v.-vis and e.p.r. spectra are in accordance with existing theories on the electronic properties of polypyrrole. While the neutral polymer is an insulator, the electrical conductivity increases to a maximum of 4×10^{-3} S cm^{-1} when the polymer is 'half' oxidized in a linear potential sweep, and then decreases to less than 10^{-4} S cm^{-1} when fully oxidized. The potential dependence of the conductivity is completely reversible. The maximum of the conductivity occurs when polarons and bipolarons have the same concentration. This supports a hopping model of the conductivity in which charge transfer occurs between polarons and bipolarons.

(Keywords: substituted polypyrrole; cyclic voltammetry; oxidation)

INTRODUCTION

Polypyrrole, which can be synthesized by oxidative polymerization of pyrrole monomers[1], can be oxidized reversibly to a polymeric salt in which the positive charge of approximately +0.3 per pyrrole ring is counterbalanced by suitable gegenions[2]. In the form of these salts, the otherwise insulating polymer becomes electrically conducting. If polypyrrole is oxidized further (i.e. to a higher potential than 1 V (vs. Ag/AgCl)), degradation usually takes place, probably initiated by the attack of nucleophiles[3].

The oxidation of polypyrrole can be investigated using potential-sweep experiments, e.g. cyclic voltammetry. By carefully avoiding the presence of nucleophiles and choosing high enough sweep rates, it is possible to substantially depress the degradation[4], but one is limited to short time studies of the higher oxidation states. We recently demonstrated that the oxidation stability of alkyl substituted polypyrroles can be enhanced by polar substitution[5]. This allows us to study oxidation states of more than 0.3 charges per pyrrole ring over a longer time-scale and in less vigorously cleaned systems than are necessary for the investigation of unsubstituted polypyrrole. In this study, we present the cyclovoltammetric investigation and *in situ* spectroscopic, gravimetric and conductivity characterization of the polar substituted polypyrrole, poly(5-acetamido-4,5,6,7-tetrahydro-2*H*-benzo[c]pyrrole) (**1**) (for the chemical structure of **1** see inset in *Figure 2*).

EXPERIMENTAL

A detailed description of the synthesis of the monomer is given in the Appendix. The polymer (**1**) was synthesized from a solution of 0.01 mol l^{-1} monomer and 0.1 mol l^{-1} tetrabutylammonium perchlorate ($TBAClO_4$) in acetonitrile. Free-standing films of the oxidized polymer of 50 μm thickness were synthesized by potentiostatic electrooxidation in a three-compartment cell at a potential of 0.9 V (vs. Ag/AgCl). Thin films for cyclic voltammetry and *in situ* spectroscopy were synthesized galvanostatically on a platinum surface. A current density of 0.2×10^{-3} A cm^{-2}, and a total charge density of 36×10^{-3} C cm^{-2} (cyclic voltammetry, *in situ* u.v.-vis) and 60×10^{-3} C cm^{-2} (*in situ* e.p.r. spectroscopy) was applied. The films were reduced to the neutral state prior to the experiments. Acetonitrile (Aldrich, 'Gold Label' grade) was used as received, and handled with strict exclusion of air. Tetrabutylammonium perchlorate ($TBAClO_4$) (Fluka) was recrystallized from ethanol, dried *in vacuo* and stored at 50°C.

*To whom correspondence should be addressed. Present address: Department of Chemical Engineering, Stanford University, Stanford, CA 94305-5025, USA

0032-3861/93/204341-06
© 1993 Butterworth-Heinemann Ltd.

Cyclic voltammograms (CVs) of the polymer deposited on a platinum surface were recorded in a 0.1 mol l^{-1} acetonitrile solution of $TBAClO_4$ with a commercial potentiostat (M173, Princeton Applied Research), using AgCl-covered Ag as a reference electrode (anodic peak potential of ferrocene = 0.4 V). For cyclovoltammetric experiments under strictly dry conditions, the polymer was synthesized on an electrode with a surface area of 0.78×10^{-2} cm^2. For *in situ* u.v.-vis spectroscopy, the polymer was deposited on a platinum-covered quartz plate with an exposed area of 0.5 cm^2. This plate served as the working electrode and was mounted parallel to two quartz windows on a home-made electrochemical cell. The spectra were recorded with a fast diode array spectrophotometer (Hewlett–Packard, HP8452A). For *in situ* e.p.r. measurements, a platinum wire of 0.4 mm diameter was covered with the polymer and inserted as a working electrode into a commercial flat electrolytic cell (Bruker, WG-810-Q). The spectra were recorded with a CW-X-band spectrometer (Bruker, ESP 300). For *in situ* gravimetric experiments, the polymer was deposited on a gold-covered surface of a circular quartz resonator. The mass of the polymer film was calculated from the frequency of the resonator[6]. The electrochemical yield of the polymerization was in agreement with an electrochemical stoichiometry of 2.3 electrons per repeat unit[1]. The amount of polymer deposited onto the electrodes in the electrochemical experiments was calculated from the total charge consumed using this stoichiometry. A two-point technique was used for *in situ* conductivity measurements[7].

RESULTS AND DISCUSSION

Figure 1 shows cyclic voltammograms (CVs) of **1** at different sweep rates. Polymer **1** was so stable that we were able to record the CV with sweep rates as low as 1 mV s^{-1}, up to potentials as high as 2 V (vs. Ag/AgCl). In all of the CVs, two anodic peaks (aI and aII (−0.1 and 1.4 V, respectively, at a scan speed of 100 mV s^{-1})) were recorded in the forward sweep, and two corresponding cathodic peaks (cI and cII (−0.2 and 0.9 V, respectively, at the same scan speed)) were recorded in the backsweep. This CV has the same features as the CV of poly(3,4-dimethylpyrrole) which has been recorded at low temperatures and high sweep rate (−70°C, 1000 mV s^{-1})[4], but by using material **1**, however, it was possible to work at room temperature and to use lower sweep rates. Integration of the CV shows that in the potential region between the two anodic peaks, the polymer has 0.33 charges per pyrrole ring, and in the 'completely oxidized' state at 1.7 V, it has 0.8 charges per ring. It was found that 90% of the charge injected into the polymer during oxidation is recovered during the reduction.

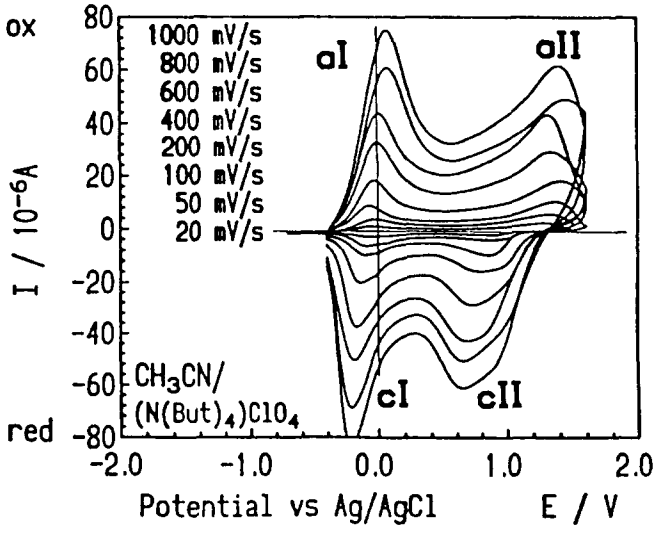

Figure 1 Cyclic voltammograms of **1**, in contact with a 0.1 mol l^{-1} solution of $TBAClO_4$ in acetonitrile, recorded at different sweep rates

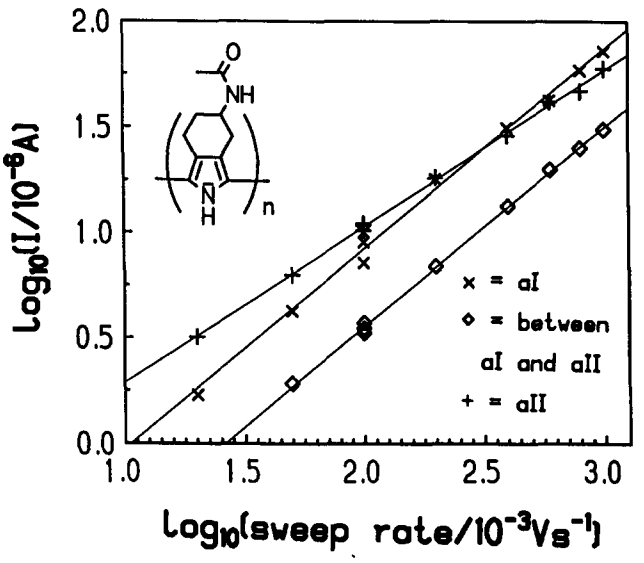

Figure 2 Double logarithmic plots of the anodic peak currents, and the lowest current between the anodic peaks, *versus* the sweep rate; slopes of the fitted straight lines are given in *Table 1*

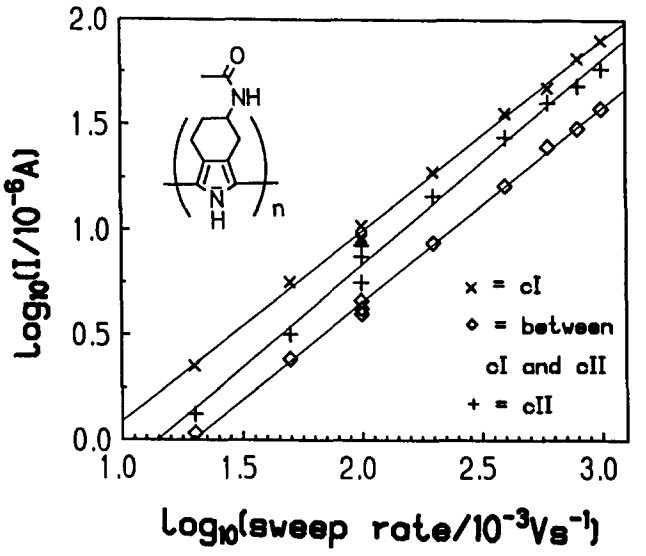

Figure 3 Double logarithmic plots of the cathodic peak currents, and the lowest current between the cathodic peaks, *versus* the sweep rate; slopes of the fitted straight lines are given in *Table 1*

Figures 2 and *3* show double logarithmic plots of the peak currents and the value of the lowest currents between the two oxidation and the two reduction peaks, *versus* the sweep rate. In this form of representation, each set of data can be fitted by a straight line, and the slopes of these lines are given in *Table 1*. In a diffusion-controlled system (e.g. redox-active species in solution) this slope is 0.5[8], while a system in which diffusion effects can be neglected (e.g. insoluble monolayers), shows a slope of

Table 1 The slopes of the straight lines fitted to the double logarithmic plots of current *versus* sweep rate, shown in *Figures 2* and *3*

Potential region of the CV	Slope of the fitted line
anodic peak (aI)	0.94
lowest current between (aI) and (aII)	0.93
anodic peak (aII)	0.73
cathodic peak (cI)	0.90
lowest current between (cI) and (cII)	0.92
cathodic peak (cII)	0.96

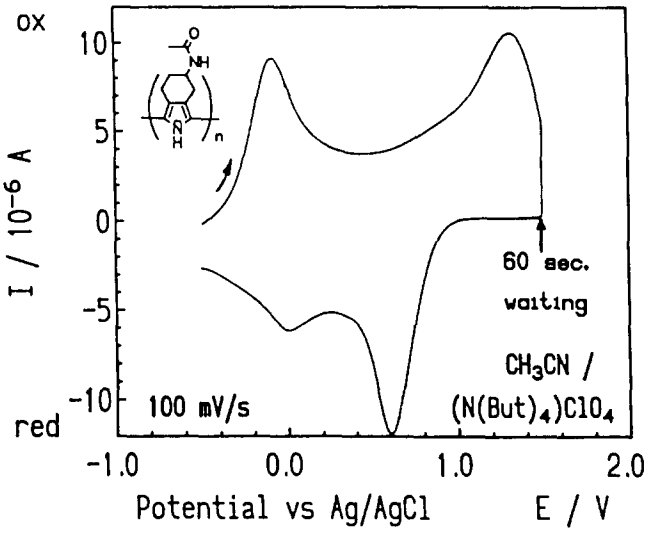

Figure 4 Cyclic voltammogram of **1**, which includes a waiting period of 60 s between forward sweep and backsweep, at a potential of 1.5 V (vs. Ag/AgCl)

1.0[9]. With one exception, the values of the slopes given in *Table 1* are between 0.90 and 0.96, which indicates that diffusion processes (in this case of the gegenions and the solvent) are not rate limiting. The line corresponding to the second anodic peak (aII), however, has a significantly lower slope, i.e. 0.73, indicating that a relatively slow diffusion or rearrangement process is involved in this stage of the oxidation. This phenomenon is also noticeable when the CV is stopped at 1.5 V (vs. Ag/AgCl) and the backsweep is carried out after a suitable waiting period (see *Figure 4*): the cathodic peak (cII) becomes higher and sharper, while the cathodic peak (cI) becomes smaller and broader without changes in the integral under the curve.

These observations might indicate that, after completion of the forward sweep, the film is still inhomogeneous but becomes more homogeneous when the slow process is completed. Similar observations have already been reported in other systems[3,10], and have been explained as being due to diffusion of gegenions[3], swelling[11], or conformational changes of the polymer chain[12].

The change in the mass of the polymer film during cyclic voltammetry was determined *in situ* with a quartz microbalance. In the absence of swelling and with only one mobile charged species, the derivative of the mass with respect to time should be proportional to the current, with the proportionality factor being the ratio of charge to mass of the mobile species. *Figure 5* shows the derivative of the mass as a function of potential. The diagram has the same general appearance as the cyclic voltammograms, except in the region of the anodic peak, aII, where the derivative of the mass is disproportionately high. With the exception of this potential region, the ratio between the derivative of the mass and the current is equal to the ratio of mass to charge of the gegenion ClO_4^- (10^{-3} g C^{-1}). It is therefore likely that in most parts of the CV, only the anion diffuses during charging or discharging, while the 'slow' process noticeable in the potential region of aII is associated with a swelling of the polymer.

U.v.-vis spectra of **1** were recorded *in situ* at regular intervals during a cyclic voltammetry scan (*Figure 6* and *Figure 7*). In the potential range of the anodic peak aI, the absorption maximum at $\lambda = 410$ nm lost intensity and shifted towards lower wavelengths. At the same time, absorptions emerged at $\lambda = 600$–500 nm and at $\lambda > 820$ nm. At a higher degree of oxidation, the absorptions at $\lambda = 600$–500 nm became weaker, while the absorption at $\lambda > 820$ nm gained in intensity, and the high energy onset of the absorption moved towards lower wavelengths. In the backsweep stage of the experiment the same spectral changes were observed, in reverse order, and at the end of the experiment the u.v.-vis spectrum was identical to that recorded at the beginning. We therefore again conclude, on the basis of these spectroscopic experiments, that no significant degradation of the polymer took place.

The observed spectral changes are in accordance with similar experiments on unsubstituted polypyrrole[13,14] and also with theories of the electronic structure of polypyrrole[15,16], with the peak at $\lambda = 410$ nm corresponding to the interband transition and the absorptions at $\lambda = 600$–500 nm corresponding to absorptions of polarons and bipolarons. At a higher degree of oxidation, the formation of a bipolaronic band should lead to a broadening of the absorption at $\lambda > 820$ nm[15]. The shifting of the high-energy onset of the absorption at $\lambda > 820$ nm towards shorter wavelengths is in agreement with this predicted broadening.

The e.p.r. spectra of **1** were also recorded *in situ* during a cyclic voltammetry scan. While the form and linewidth of the spectra were not affected, the intensity (= double integral of the e.p.r. signal) changed with the applied

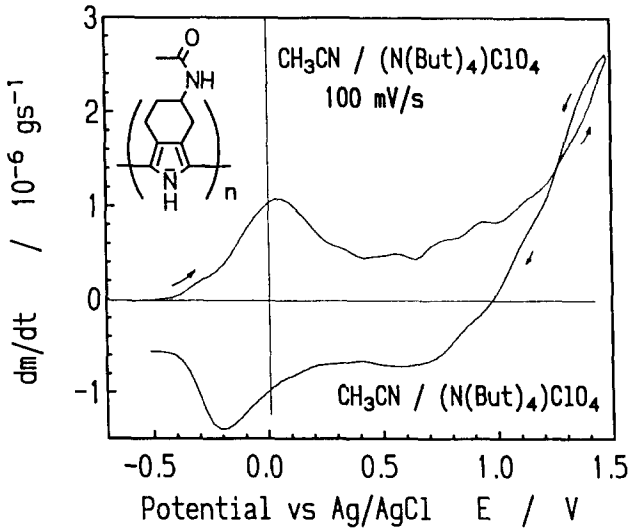

Figure 5 Derivative of the mass with respect to time of a film of **1** measured *in situ* during a cyclic voltammetry scan, plotted as a function of potential (sweep rate = 100 mV s^{-1})

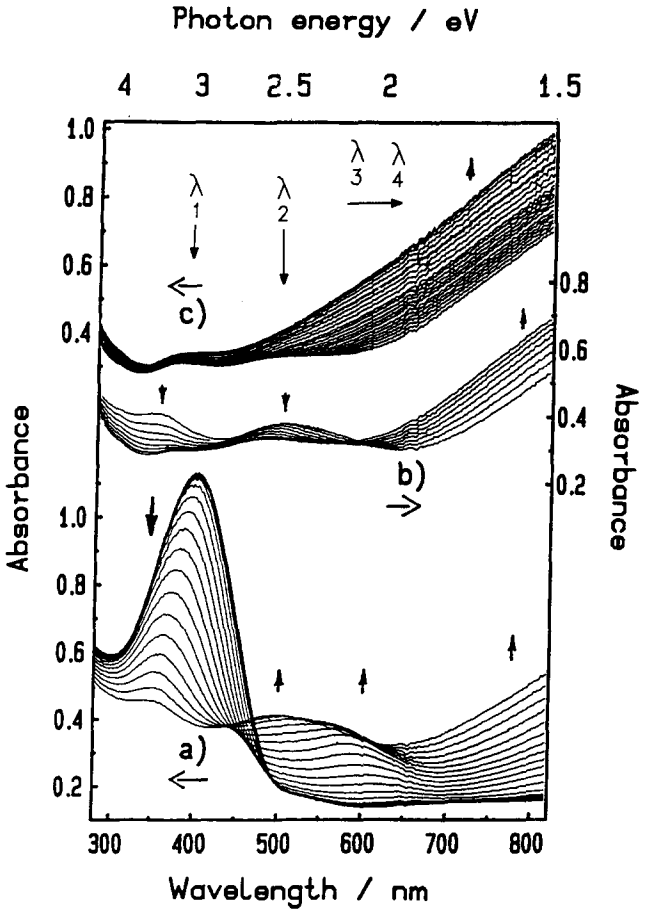

Figure 6 U.v.-vis spectra of **1** recorded at intervals of 0.04 V during the forward sweep of a cyclic voltammetry scan (sweep rate = 20 mV s^{-1}). For clarity the spectra are divided into three groups: (a) potential range of the anodic peak aI (−0.8 to +0.36 V); (b) potential range between peaks aI and aII (0.36 to 0.64 V) and; (c) potential range of the anodic peak aII (0.68 to 1.5 V). Arrows indicate the change of the spectra during oxidation

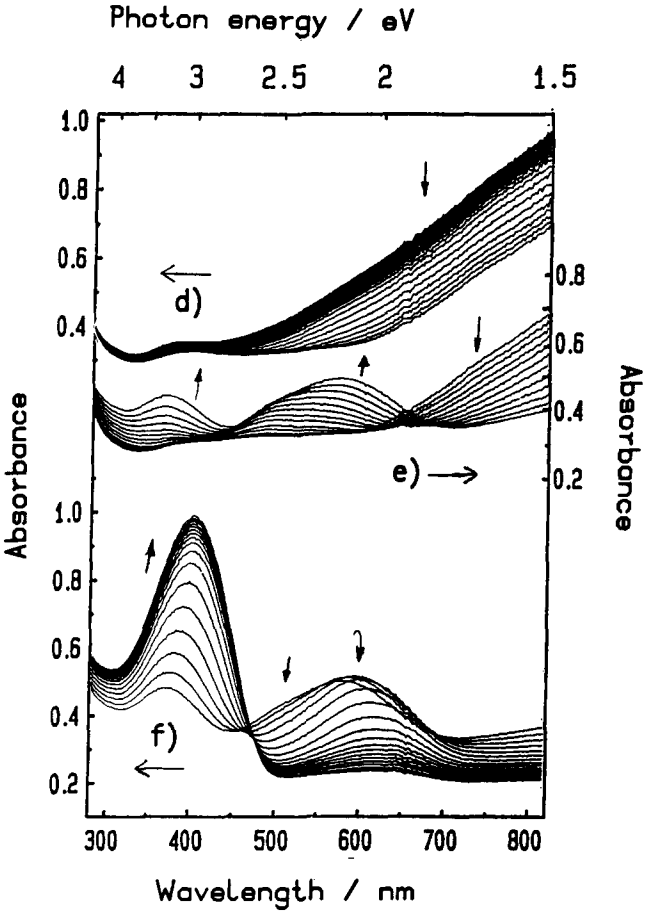

Figure 7 U.v.-vis spectra of **1** recorded at intervals of 0.04 V during the back sweep of a cyclic voltammetry scan (sweep rate = 20 mV s^{-1}). For clarity the spectra are divided into three groups (cf. *Figure 6*): (d) potential range of the cathodic peak cII (1.5 to 0.3 V); (e) potential range between peaks cI and cII (0.26 to −0.18 V) and; (f) potential range of the cathodic peak cI (−0.18 to −0.8 V). Arrows indicate the change of the spectra during reduction

potential. The intensity is shown in *Figure 8* as a function of the applied potential. The spin density has its maximum in the region of the anodic peak aI and decreases upon further oxidation, with the 'completely' oxidized state at 1.5 V (vs. Ag/AgCl) being virtually spinless. These results are in accordance with both the u.v.-vis spectroscopic results and theories of the electronic structure of polypyrrole, which predict a spinless bipolaronic band in the 'completely' oxidized state. In the potential region between the two oxidation peaks, the spin density was found to be half of the maximum value. Therefore, half of the polarons have been converted to bipolarons at this point. This interpretation is in agreement with the degree of oxidation, assuming a (bi)polaron extends over approximately four pyrrole rings[15].

Figure 9 shows the conductivity (σ) of **1** measured *in situ* during a cyclic voltammetry scan. Starting from the neutral polymer, σ initially increases with oxidation, reaches its peak value at a potential between the two oxidation peaks, and then decreases again when the polymer is oxidized further. In the backsweep stage, σ reaches the same maximum value as during the forward sweep, reflecting the complete reversibility of the oxidation process. The hopping model of electrical conductivity implies that in the polymeric salt the charge is transferred between localized sites. This charge transfer can in principle be of a disproportion

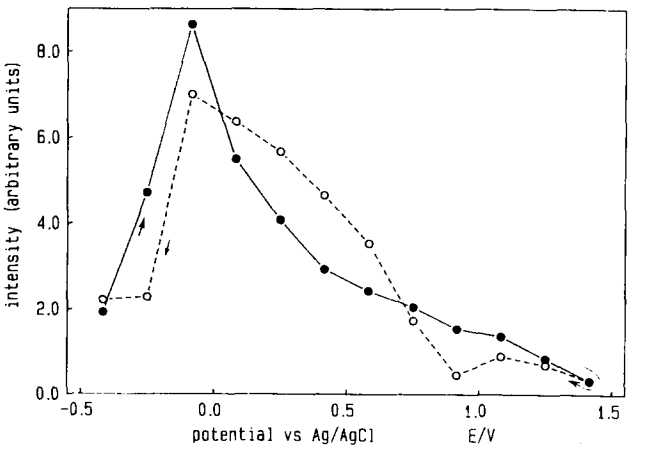

Figure 8 The intensity of the e.p.r. signal of **1**, as a function of the applied potential, measured *in situ* during a cyclic voltammetry scan (sweep rate = 20 mV s^{-1})

type (e.g. $A^+ + A^+ \rightarrow A^{0+} + A^{2+}$), where two polarons combine to form a bipolaron, or of an exchange type[17] (e.g. $A^+ + A^{2+} \rightarrow A^{2+} + A^+$) where an electron is transferred from a polaron to a bipolaron. The u.v.-vis and the e.p.r. spectroscopic experiments indicate the presence of polarons and bipolarons, and also that they both have the same concentration when the

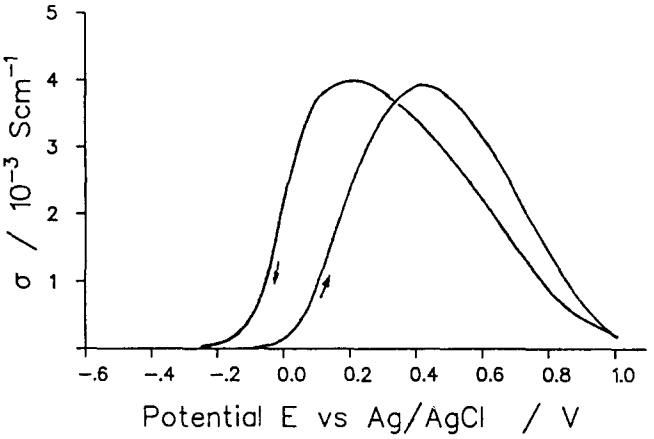

Figure 9 Conductivity of **1**, as a function of the applied potential, measured *in situ* during a cyclic voltammetry scan (sweep rate = 1 mV s^{-1})

conductivity reaches its maximum value. Therefore, our data support a hopping mechanism in which the conductivity occurs through charge transfer between polarons and bipolarons.

ACKNOWLEDGEMENTS

We thank V. Enkelmann for fruitful discussions and C. Huth and C. Sieber for significant technical assistance.

REFERENCES

1 Genies, E. M., Bidan, G. and Biaz, A. F. *J. Electroanal. Chem.* 1983, **149**, 101
2 Pfluger, P., Weiser, G., Scott, J. C. and Street, G. B. in 'Handbook of Conducting Polymers', (Ed. T. A. Skotheim), Marcel Dekker, New York, 1986, p. 859
3 Wernet, W. and Wegner, G. *Makromol. Chem.* 1987, **188**, 1465
4 Ofer, D., Crooks, R. M. and Wrighton, M. S. *J. Am. Chem. Soc.* 1990, **112**, 7869
5 Goedel, W. A., Enkelmann, V. and Wegner, G. *Synth. Met.* 1991, **41**, 377
6 Rosenmund, J. and Schlinder, R. N. *Synth. Met.* 1991, **43**, 2967
7 Schiavon, G., Sitran, S. and Zotti, G. *Synth. Met.* 1989, **32**, 209
8 Bard, A. J. and Faulkner, L. R. 'Electrochemical Methods', Wiley, New York, 1980, p. 218
9 Anson, F. C. *Anal. Chem.* 1977, **49**, 1589
10 Odin, C. and Nechtschein, M. *Synth. Met.* 1991, **43**, 2943; 1991, **44**, 177
11 Kaufmann, F. B. *J. Am. Chem. Soc.* 1980, **102**, 483
12 Heinze, J., Bilger, R. and Meerholtz, K. *Ber. Bunsenges. Phys. Chem.* 1988, **92**, 1266
13 Yakushi, K., Lauchlan, L. J., Clarke, T. C. and Street, G. B. *J. Chem. Phys.* 1983, **79**, 4774
14 Kaufmann, J. H., Colaneri, N., Scott, J. C., Kanazawa, K. K. and Street, G. B. *Mol. Cryst. Liq. Cryst.* 1985, **118**, 171
15 Bredas, J. L. *Mol. Cryst. Liq. Cryst.* 1985, **118**, 49
16 Scott, J. C., Bredas, J. L., Kaufmann, J. H., Pfluger, P., Street, G. B. and Yakushi, K. *Mol. Cryst. Liq. Cryst* 1985, **118**, 163
17 Zotti, G. and Shiavon, G. *Synth. Met.* 1989, **31**, 347; 1991, **41**, 445: *Chem. Mater.* 1991, **3**, 62
18 Kornfeld, E. C. and Bach, N. J. US Patent 4 235 776, 1980

APPENDIX

Synthesis of monomer

5-Acetamido-4,5,6,7-tetrahydro-2*H*-benzo[c]pyrrole was synthesized from 4-aminocyclohexanol in a variation of the procedure of Kornfeld and Bach[18] in four steps; steps 2–4 were carried out under an inert gas atmosphere.

Step 1: synthesis of 4-acetamidocyclohexanone. A solution of 230.4 g (2 mol) of 4-aminocyclohexanol in 230 ml of water was mixed with 182 g (2.2 mol) of sodium bicarbonate. The mixture was stirred, cooled with ice, and then 210 ml (2.2 mol) of acetic anhydride were added dropwise over 30 min. The mixture was then slowly heated to 80°C, and after a period of 2 h was cooled again with ice. The temperature was kept below 30°C while first 117 ml (2.2 mol) of concentrated sulfuric acid, and then a mixture of 220 g (2.2 mol) of CrO_3, 150 ml of water and 190 ml of H_2SO_4 was slowly added. After 10 min, 20 ml of isopropanol were added to destroy any excess of Cr(VI), and after a further 10 min 1.5 l of water were added and the mixture was then extracted in a liquid/liquid extractor using ethyl acetate. The crude product was dissolved in hot toluene (20 ml per g of solid), decanted from the insoluble oil and recrystallized at −20°C. The insoluble oil was extracted with boiling toluene to give additional product. The yield was 180–200 g (1.2–1.3 mol) (60–65%).

Elemental analysis: calculated for $C_8H_{13}O_2N$, C 61.92, H 8.44, N 9.03, O 20.61; found, C 62.00, H 8.45, N 8.91, O 20.52. ^{1}H n.m.r. ($CDCl_3$) δ: 6.25 (s, 1H, CO–NH), 4.16 (m, 1H, CO–NH–CH–$(CH_2)_2$), 2.37 (m, 4H, CO–CH_2–C), 2.15 and 1.15 (m, 2H, NH–CH–CH_2–C), 1.92 (s, 3H, CH_3). ^{13}C n.m.r. ($CDCl_3$) ppm: 210.0 ($(CH_2)_2$–CO), 169.5 (CH_3–CO–NH), 46.3 (NH–CH–$(CH_2)_2$), 39.0 (CO–CH_2–CH_2), 31.5 (NH–CH_2–CH_2), 23.5 (CH_3). I.r. (KBr) cm^{-1}: 3295 (s, ν(N–H)), 3060 (w, 2nd harmonic of amide II), 2940 (m, $\nu(CH_3)$), 2850 (w, $\nu_s(CH_2)$), 1720 (s, ν(C=O)), 1650 (s, amide I), 1550 (s, amide II), 1450 (m), 1370 (m), 1200 (s), 605 (m).

Step 2: synthesis of 4-acetamido-2-[(dimethylamino)-methylene]cyclohexanone. 75.6 g (0.5 mol) of 4-acetamidocyclohexanone were mixed with 1.2 l of dry toluene, 168 ml (1.25 mol) of *N,N*-dimethylformamide dimethyl acetal (Fluka) and 7 ml (0.5 mol) of triethylamine. A pressure equalizing funnel was filled with 160 g of molecular sieve (0.4 nm) and mounted between the flask containing the mixture and a condenser. The mixture was refluxed for 45 min, with the condensate flowing back to the reaction mixture through the molecular sieve. The solution was then concentrated to 200 ml and the bulk of the product was then precipitated by slowly cooling to room temperature. The mixture was filtered, the remaining solution concentrated and the residue was then fractionated by flash chromatography with silica gel, using a mixture of 80 vol% acetone, 19 vol% methanol and 1 vol% triethylamine to yield additional product. The yield was 70–80 g (0.33–0.38 mol) (65–75%).

Elemental analysis: calculated for $C_{11}H_{18}O_2N_2$, C 62.83, H 8.63, N 13.23, O 15.22; found, C 62.38, H 8.43, N 13.10, O 15.29. ^{1}H n.m.r. ($CDCl_3$) δ: 7.42 (s, 1H, C=CH–N), 6.60 (d, 1H, CO–NH–CH), 4.05 (m, 1H, NH–CH–$(CH_2)_2$), 3.03 (s, 6H, N–CH_3), 2.48 (q, 2H, CO–CH_2–C), 2.35 (m, 2H, NH–CH–CH_2–C=C), 1.92 (s, 3H, CH_3), 1.25 (m, 2H NH–CH–CH_2–CH_2–). ^{13}C n.m.r. ($CDCl_3$) ppm: 195.5 ($(CH_2)_2$–CO–C=C), 169.5 (CH_3–CO–NH), 151.6 (CO–C=CH–N$(CH_3)_2$), 100.5 (CO–C=CH–N$(CH_3)_2$), 45.8 (NH–CH–$(CH_2)_2$), 43.0 (–N$(CH_3)_2$), 36.0, 32.5, 28.1 (–CH_2), 23.5 (CH_3). I.r. (KBr) cm^{-1}: 3300 (s, ν(N–H)), 3060 (w, 2nd harmonic of amide II), 2940 (m, $\nu(CH_3)$), 2910 (w, $\nu_{as}(CH_2)$), 2890

(w, ν(CH)), 2850 (w, $\nu_s(CH_2)$), 1640 (s, amide I), 1530 (s, amide II), 1410 (s), 1370 (s), 1350 (m), 1270 (s), 1105 (m), 995 (m), 955 (m), 855 (m), 610 (m).

Step 3: synthesis of 2-acetyl-5-acetamido-4,5,6,7-tetrahydro-2H-benzo[c]pyrrole. 3.9 g (0.1 mol) of potassium were dissolved in 150 ml of dry ethanol and 8.25 g (0.11 mol) of glycine were added. The solution was stirred overnight, filtered, mixed with 21.0 g (0.1 mol) of 4-acetamido-2-[(dimethylamino)methylene]cyclohexanone and refluxed for 105 min. After cooling to room temperature, 850 ml of diethylether were slowly added. The white precipitate was filtered off, dried for 1 h at a pressure of 0.3×10^2 Pa, mixed (under an inert gas atmosphere) with 150 ml of acetic acid anhydride (freshly distilled from 0.4 nm molecular sieve), and refluxed for 1 h. The mixture was then concentrated and the solid residue was fractionated by flash chromatography with Florisil (Fluka) using a gradient eluent, starting with a mixture of 1 vol% and ending with a mixture of 7 vol% of methanol in chloroform. The crude product was dissolved in dichloromethane (5 ml per g of solid) and reprecipitated by the dropwise addition of diethyl ether. The yield was 5–7 g (0.02–0.03 mol) (20–30%).

Elemental analysis: calculated for $C_{12}H_{16}O_2N_2$ (220.27 g mol^{-1}), C 65.43, H 7.32, N 12.72, O 14.53; found, C 65.49, H 7.34, N 12.63, O 14.50. M.s. (70 eV) *m/z* (%): 221 [M+H] (1.9), 220 $[M]^+$ (1.9), 177 [M−(CO–CH_3)] (1.7), 161 [M−(NH=COH–CH_3)] (99.8), 135 [M−(CH_2=CH–NH–CO–CH_3)] (4.8), 119 [M−(NH=COH–CH_3–CH_2=CO)] (81.3), 118 [M−(NH=COH–CH_3–CO–CH_3)] (72.0), 93 [M−(CH_2=CH–NH–CO–CH_3–CH_2=CO)] (22.8), 43 $[CO–CH_3]^+$ (16.6). ^{1}H n.m.r. ($CDCl_3$) δ: 6.89 (s, 2H, α-pyrrole-H), 6.15 (s, 1H, CO–NH–CH–), 4.10 (m, 1H, CO–NH–CH–(CH_2—)$_2$), 2.58 (m, 2H, pyrrole–CH_2–CH_2), 2.72, 2.32, 1.80 and 1.60 (m, 4H, NH–C*H–CH_2–CH_2 and NH–C*–CH_2– pyrrole), 1.92 (s, 3H, CH_3). ^{13}C n.m.r. ($CDCl_3$) ppm: 169.7 (CH_3–CO–NH), 167.4 (CH_3–CO–pyrrole), 123.43, 122.9 (β-C of the pyrrole ring), 115.1, 114.5 (α-C of the pyrrole ring), 45.6 (NH–CH–$(CH_2)_2$), 28.8, 28.5, 19.3 (CH_2), 23.3, 22.0 (CH_3). I.r. (KBr) cm^{-1}: 3300, 3260 (broad, s, ν(N–H)), 3080 (w, 2nd harmonic of amide II), 2950 (w, $\nu(CH_3)$), 2920 (w, $\nu_{as}(CH_2)$), 2850 (w, $\nu_s(CH_2)$), 1710 (s, ν(CO–pyrrole), 1635 (s, amide I), 1540 (s, amide II), 1410 (s), 1370 (s), 1350 (m), 1060 (m), 945 (m), 945 (m), 790 (m), 610 (m).

Step 4: synthesis of 5-acetamido-4,5,6,7-tetrahydro-2H-benzo[c]pyrrole. 5.5 g (0.025 mol) of 2-acetyl-5-acetamido-4,5,6,7-tetrahydro-2*H*-benzo[c]pyrrole were dissolved in 50 ml of hydrazine hydrate and refluxed for 10 min. The solution was concentrated and the solid residue was then fractionated in a sublimation apparatus, first at 100°C (0.3×10^2 Pa) to remove acethydrazide, and finally at 120°C (0.3×10^2 Pa). The yield was 3.5–4 g (0.019–0.022 mol) (78–88%).

Elemental analysis: calculated for $C_{10}H_{14}ON_2$ (178.23 g mol^{-1}), C 67.39, H 7.92, N 15.72, O 8.98; found, C 67.35, H 7.91, N 15.77, O 9.03. M.s. (70 eV) *m/z* (%): 179 [M+H] (6.0), 178 $[M]^+$ (1.7), 135 [M−(CO–CH_3)] (4.6), 119 [M−(NH=COH–CH_3)] (99.9), 93 [M−(CH_2=CH–NH–CO–CH_3)] (42.5), 43 $[CO–CH_3]^+$ (17.2). ^{1}H n.m.r. ($CDCl_3$) δ: 8.2 (s, NH–pyrrole), 6.5 (d, 2H, α-pyrrole–H), 5.6 (s, 1H, CO–NH–CH–), 4.23 (m, 1H, CO–NH–CH–$(CH_2–)_2$), 2.65 (m, 2H, pyrrole–CH_2–CH_2), 2.93, 2.46, 1.90 and 1.82 (m, 4H, NH–C*H–CH_2–CH_2 and NH–C*H–CH_2–pyrrole), 1.92 (s, 3H, CH_3). ^{13}C n.m.r. ($CDCl_3$) ppm: 169.5 (CH_3–CO–NH), 117.8, 116.6 (β-C of the pyrrole ring), 113.9, 113.3 (α-C of the pyrrole ring), 45.8 (NH–CH–$(CH_2)_2$), 29.0, 28.7, 18.9 (CH_2), 23.5 (CH_3). I.r. (KBr) cm^{-1}: 3380, 3290 (s, ν(N–H)), 3080 (w, 2nd harmonic of amide II), 2920 (s, $\nu_{as}(CH_2)$), 2850 (m, $\nu_s(CH_2)$), 1640 (s, amide I), 1540 (s, amide II), 1440 (m), 1370 (m), 1310 (m), 1060 (m), 775 (m).